Astron. Astrophys. 330, 243–252 (1998)

ASTRONOMY
AND
ASTROPHYSICS

On the spectacular variations of Be stars

Evidence for a temporarily tilted circumstellar disk

W. Hummel

Universitätssternwarte München, Scheinerstr. 1, D-81679 München, Germany

Received 27 January 1997 / Accepted 15 September 1997

Abstract. A new explanation for the spectacular emission line variations occuring in the Be stars γ Cas and 59 Cyg is presented. We propose a circumstellar Keplerian disk, tilted with respect to the equatorial plane. The precessing nodal and apsidal line causes a variation in the emission line widths and profile shapes. In particular the sequence of alternating shell-phases and narrow single-peak phases is proposed to be due to an apparent variation in the disk inclination.

Key words: line: formation; line: profiles; stars: circumstellar matter; stars: emission-line, Be; stars: individual: γ Cas ; stars: individual: 59 Cyg

1. Introduction

Be stars are fast rotating early-type main-sequence stars, which have shown Hα in emission at least once. The optical and IR emission lines as well as the IR continuum excess of Be stars is due to a cool gaseous Keplerian disk in the equatorial plane of the central star (see Waters & Marlborough 1994 for a review). One of the main pieces of evidence for this model is the correlation between the stellar projected rotation velocity $v \sin i$ and the emission line widths FWHM (Struve 1931, Slettebak & Reynolds 1978). In addition, the bottom widths $\Delta V_{\rm tot}$ of the faint Fe II emission lines, which are not contaminated by electron scattering or by an underlying stellar absorption profile, correlate more strongly with the stellar $v \sin i$ (Hanuschik 1987). Be stars with very large $v \sin i$ are seen equator on and consequently the edge-on circumstellar disk can absorb and redistribute a considerable fraction of the stellar radiation giving rise to UV-continuum depression (Beekmans 1976) and the so-called shell-lines with a deep central depression below the local stellar continuum.

Emission lines of Be stars are variable. The monitoring of the circumstellar emission lines indicate variations in equivalent width and line profile shape (e.g. Dachs 1987; Hubert 1994). A frequently observed type of emission line variability is the quasi-cyclic long-term V/R-variations with a typical cycle-time of 5-10 years. These are due to m = 1 density waves in a perturbed circumstellar disk (Okazaki 1991; Papaloizou et al. 1992; Hanuschik et al. 1995; Telting et al. 1994; Hummel & Hanuschik 1997).

A very rare kind of emission line variation are the shell events, sometimes called the Be – Be-shell phase transitions. There are at least three Be stars known to have shown such phase transitions: γ Cas (Baldwin 1939, Edwards 1956 and references therein), 59 Cyg (Doazan 1975; Hubert-Delpace & Hubert 1981; Barker 1982), and Pleione (Gulliver 1977; Hirata & Kogure 1978). The long-term variation of these three stars is reviewed by Kogure & Hirata (1982).

Two of these Be stars, namely γ Cas and 59 Cyg, showed two successive shell events, which were associated with a remarkably synchronous quasi-cyclic *variation of the emission line width* in all observed emission lines, called *spectacular variation* (SV; Doazan et al. 1983).

A variation of the emission line width removes the correlation between $v \sin i$ and the FWHM and consequently a circumstellar equatorial disk fails to explain the spectacular variations (hereafter SV). Early attempts to model the SV of γ Cas focused on the colour temperature variation of the underlying star (Baldwin 1940; Lockyer 1933; Barbier 1948) and are mostly based on the photometric light curve of Huffer (1938) and Lockyer (1933). Goraya & Tur (1988) argue for mass loss events forming two recurrent thick shells. Recently, Marlborough (1997) noted the similarity between the photometric variability of γ Cas and that of LBVs.

In this study we analyze the SV of γ Cas in particular the tabulated variation of the emission line parameters (Baldwin 1939), in order to extract kinematical constraints on the circumstellar emitting gas. In Sect. 2. we summarize the observations. A new interpretation is given in Sect. 3, some aspects of which are tested in Sect. 4. The conclusions are drawn in Sect. 5.

2. Observations and properties of spectacular variations

2.1. γ Cas

γ Cas (HR 264, HD 5394, MK=B0IVe, $v \sin i$ = 300 km s^{-1}) was the first Be star to be detected (Secchi 1867) and is the vi-

sually brightest in the northern hemisphere. The emission line spectrum of γ Cas was rather constant from its detection in 1866 till the first observed variations in 1928. These early observations were eye-estimates and are critically discussed by Lockyer (1933) and Edwards (1944). The first significant variation in the emission line profile shapes was detected in 1928, when the V/R-ratio (the continuum-subtracted intensity ratio of the violet to the red emission peak $(I_V - I_C)/(I_R - I_C)$) of Hβ and Hγ which had been unity to that point gradually decreased (McLaughlin 1937). These V/R variations became cyclic (See Table 1). We will call this time interval (1928-1934) with ordinary long-term V/R-ratio variations, epoch A. Some years later, in early 1934, the emission line width also became variable and the line profile shapes changed twice from ordinary double-peak to single-peak and shell-profiles (Baldwin 1939). The two phase transitions, shell to single-peak, show a stronger violet peak, the phase transitions from single-peak to shell show symptomatically stronger red peaks. This epoch (1934-1940) with emission width variations (=SV) will be called epoch B.

In 1939, during the last shell phase which indicates the end of the SV the emission faded and a quasi-normal B-type spectrum with only traces of emission in Hα and Hβ was visible. The spectral evolution of γ Cas after 1940 (= after the SV) is indistinguishable from other 'normal' Be stars. From 1940 onwards until 1969 the traces of emission increased slowly and continuously. The emission lines were symmetric. In 1969 long-term quasi-periodic V/R variations, a typical phenomena also observed in many other Be stars started and still continue (e.g. Doazan et al. 1983). None of its current spectral features betrays the exceptional variations between 1934 and 1940.

The present long-term V/R-variations of γ Cas which started in 1969 are neither accompanied by a variation of emission widths nor by the appearance of single-peak or shell-profiles.

2.2. 59 Cyg

59 Cyg (HR 8047, B1.5Vnne, $v \sin i$ = 370 km s^{-1}) also showed two shell phases, the first in June 1973 (Doazan 1975) and a second from Dec. 1974 to April 1975 (Hubert-Delplace & Hubert 1981; Barker 1982)

As in the case of γ Cas V was greater than R during the phase transition shell – single-peak and V was smaller then R in the succeeding phase transition single-peak – shell. During the shell phase, shell profiles became visible in the higher Balmer emission lines down to Hβ, while the Hα profile only decreased in strength.

The SV of 59 Cyg have been partly monitored with the S 2/68 spectroscopic UV telescope and the IUE satellite. These UV observations show a decrease in the UV flux during the second shell phase (Beekmans 1976; Marlborough & Snow 1980; Doazan et al. 1989). Moreover the UV flux increased again during the fading of the shell phase (Doazan et al. 1994). Such an important anti-correlation between optical and UV data is also documented for another Be star with Be – Be-shell phase transitions: Pleione (Doazan et al. 1987) indicating that shell phases of normal Be stars (not accompanied by a variation of emission widths) and shell phases during SV originate from the same physical or geometric conditions. In both cases the stellar surface is more obscured by the circumstellar rotating gas than during Be phases without shell characteristics in their spectra.

2.3. Limits on the observations

The observations interpreted in this study are the figures and tables based on the photographic plates of the Michigan Observatory recorded between January 6 1927 (JD=2424887) and August 1940 (JD=242 9846) and discussed in detail by Baldwin (1939, 1940, 1941; hereafter B1, B2, B3), McLaughlin (1937) and Cleminshaw (1936). In the following we will concentrate on the SV of γ Cas alone, because of the higher resolution of the data with respect to 59 Cyg and the incomparably larger coverage of the time interval.

For convenience we define

$$t = \text{Julian date} - 2\,420\,000 \text{ days} \quad (1)$$

According to the recorded Hδ emission line shapes (B1, Fig. 1-3) and the emission line parameters of He I, Fe II, Si II and Mg II the great outburst (epoch B, 1934-1940) can be roughly divided into four stages: first narrow-line stage, first shell phase, second strong narrow-line phase and finally the second strong shell phase. The evolution of the spectrum is tabulated in Table 1. The observations were recorded using photographic plates with a dispersion of 25 Å/mm. No information is given about the intensity of the clear plate or a possible correction of the exposure sensitivity. Linearity in the exposure intensities is not proven. Cleminshaw defines his $V_{\rm edge}$ values as the radial velocity at the red (blue) edge of the red (blue) emission peak. It should be noted that the radial velocity values $V_{\rm edge}$ of Baldwin are not the velocities at the bottom edge of the profiles $V_{\rm tot}$, as presently used as diagnostic tools. According to B3 (his Fig. 1) $V_{\rm edge}$ is measured in the wings of the emission lines and is therefore closer to the FWHM than to the total width $\Delta V_{\rm tot}$ of the line profiles. Therefore Baldwin's (after t = 8000) and Cleminshaw's edge values consist of different systematic errors, based on the subjective measurement errors. Thus, $V_{\rm edge}$ before t = 8000 are systematically larger than those after t = 800. We estimate the spectral resolution to be better than the FWHM of the Hδ profile during the second narrow-width phase: $R \gg 6000$

In this paper we focus our attention on the synchronous variation of the emission line shapes of γ Cas during the great outbursts in the thirties in order to derive kinematical constraints on the circumstellar gas.

3. Interpretation

The symmetric double-peak emission lines of γ Cas before and after the outbursts are comparable to those of other Be stars in shape and variability. The spectrum has been modelled for the epoch 1972 and the emission lines, the continuum radiation and the line polarization show strong evidence for an equatorial

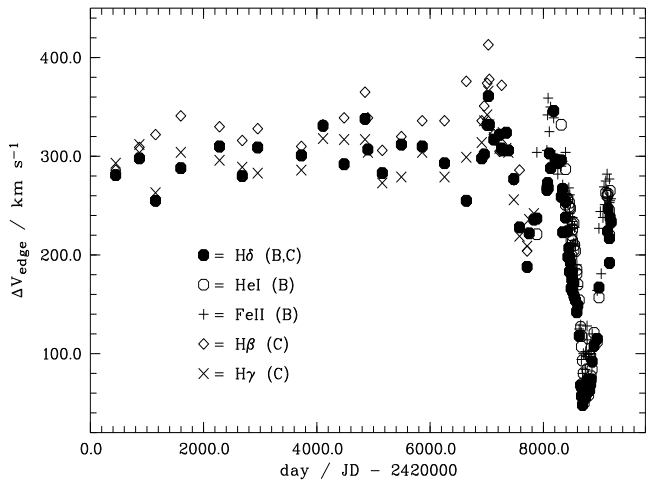

Fig. 1. Evolution of $\Delta V_{\rm edge}$ from 1914 onwards for several emission lines. Data collected from Cleminshaw (1936) covering the epoch JD=24200000-2428000 (Index C) and Baldwin (1941) for data after JD=2428000 (Index B).

circumstellar disk (Poeckert & Marlborough 1978). The long-term quasi-cyclic V/R variations (after 1969) are due to global disk oscillations (Okazaki 1991).

3.1. Influence of the scale height H(R)

A reasonable approach would be to explain the shell events by a variation of the disk height H or the meridional half opening angle Θ, as proposed by Kogure et al. (1978) and by Hanuschik (1996) for the shell events of Pleione during 1977. Pleione ($v \sin i$ = 400 km s^{-1}) is expected to be seen at large inclination $i \simeq 70^\circ$. Such a purely geometrical variation of the disk size ($R_{\rm d}$) or shape (Θ) is certainly applicable to shell events without emission width variations in general as in the case of Pleione. However, a variation of Θ or $H(R)$ *alone* cannot account for the observed narrow-line phases during SV as occured in γ Cas and 59 Cyg. In the case of γ Cas with an inclination of $i = 45^\circ$ (Quirrenbach et al. 1993) the meridional disk half opening angle has to increase from $\Theta \simeq 13^\circ$ up to at least $\Theta = 45^\circ$ in order to obscure a considerable fraction of the stellar surface to produce shell emission lines. On the other side, a decrease of Θ does not result in single-peak emission lines.

3.2. Influence of the disk radius

One could also think of a very large increase in the emission disk radius resulting in stronger emission lines with a smaller peak separation, finally producing single-peaked emission lines with a smaller FWHM but unique $\Delta V_{\rm tot}$. For a limited interval of inclinations around $i \simeq 70^\circ$ such a variation of disk radius can also result in shell events for metallic lines (Hanuschik 1996). Again, the inclination of γ Cas is too low for shell events due to the disk radius.

Table 1. Evolution of the Hδ emission line of γ Cas during the spectacular variations. P_Ω denotes the cycle time for the emission line width variation. $P_{\rm V/R}$ denotes the cycle time for the V/R-ratio variations.

day JD[a)]	day JJMMDD	V/R	Ω	$\tilde{\omega}$[d)]
before	1928	$V \simeq R$		
	1929	$V > R$[b)]		$\frac{\pi}{2}$
	1930	$V = R$[b)]		
6201 >	311205	$V \simeq R$		
6639	320310	$V < R$		$\frac{3\pi}{2}$
6959	320908	$V > R$		$\frac{\pi}{2}$
7578	340519	$V < R$		$\frac{3\pi}{2}$
7785	341212	single[c)]	$\frac{3\pi}{2}$	
7885	350322	$V > R$		$\frac{\pi}{2}$
8256	360327	shell	$\frac{\pi}{2}$	
8434	360921	$V < R$		$\frac{3\pi}{2}$
8799	370921	single[c)]	$\frac{3\pi}{2}$	
9419	380603	$V > R$		$\frac{\pi}{2}$
9705	400315	shell	$\frac{\pi}{2}$	
	> 1940	no emission		
	> 1941	$V = R$		
since	1969	cyclic V/R		

Notes:
a) + 2 420 000
b) from Lockyer (1933)
c) peak
d) anti-clock wise orbital motion

3.3. Radial velocities

One possibility to overcome this problem would be to assume a geometry or a kinematical structure different from that of a rotating disk.

In this case any net radial motion of the circumstellar material would be visible by a radial velocity shift of the narrow absorption during the shell events. The observed radial velocities of the central shell depression ($V_{\rm cd}$) are given as -43 km s^{-1} , -44 km s^{-1} , and -15 km s^{-1} for Hδ, He I and Fe II during the first shell phase respectively. The values of Si II and Mg II can be interpolated to be smaller than -16 km s^{-1} (B1). McLaughlin (1937) also gives -41 km s^{-1} , and -44 km s^{-1} for Hδ and He I.

The radial velocity of the central depression (the most optically thick part of the line profile) reflects the projected velocity with the smallest velocity gradient along the line-of-sight. These values are in the range of typical radial velocities of asymmetric shell profiles of other Be stars such as 48 Lib, which are believed to be generated in circumstellar rotating disks. The shell emission lines do not support a possible kinematical structure distinctly different from normal Be shell stars. In particular the velocity of the shell depression does not support this in the outer parts of the disk.

3.4. Stellar variations

γ Cas has also shown variations in brightness and colour. Observations earlier than the second single-peak phase are incomplete but suggest that the star was constant in brightness $V = 2\overset{\mathrm{m}}{.}1$. After $t = 8500$, the brightness rose to $V = 1\overset{\mathrm{m}}{.}57$ at t=8662 and faded during the second single-peak (Fig. 6). From $t > 9700$ onward, the light-curve of γ Cas was more or less constant with $V \simeq 2\overset{\mathrm{m}}{.}8$ (Huffer 1938; Howarth 1979).

Greaves & Martin (1936) give colour temperatures of T=10 500 K in 1936 November ($V > R$) and T=9 200 K around the second narrow-line stage, while they found T=16 100 K in 1926 before the SV begun. B2 argues for a cyclic expansion of the stellar radius by a factor of two combined with a cooling of the outer layers of the stellar atmosphere. Indeed B2 found that the Hδ stellar absorption profile narrowed by a factor of two during the second single-peak stage, in agreement with a larger stellar radius under the assumption of angular momentum conservation ($V \sim R^{-1}$). Since the Keplerian rotation of the circumstellar gas varies as $V_{\mathrm{K}} \sim R^{-\frac{1}{2}}$ we can expect a narrowing of the emission lines by a factor $2^{-\frac{1}{2}}$ during the single-peak stage, where the inner disk parts are swallowed by the expanding star. Observed ΔV_{edge}-variations, however, vary by more than a factor of three. Hence a possible stellar expansion is insufficient to account for the observed emission line width variations. A further weak point of such a scenario is the expectation that faint emission lines like He I or Fe II, which are mostly formed in the inner disk regions, should weaken or disappear during the narrow-line stage. The observations show that the opposite is true.

We cannot fully exclude that possible stellar variations are the origin of SV or have at least a strong impact on the SV. However, since we are mainly interested in the geometrical and kinematical evolution of the circumstellar gas, we concentrate our efforts on the variations of the emission lines alone and assume that the impact of possible stellar variations can be neglected.

Our main argument to favour a kinematical/geometrical scenario is that all emission lines of hydrogen, ionized metals and of neutral helium vary synchronously in intensity and profile shape according to B2 and B3. A variation of the disk temperature or the density would change the ionisation structure of the disk. According to B3, there are no indications for strong anti-correlations among the line intensities of different species.

3.5. Model construction

From the morphological point of view, the narrow-line spectrum of γ Cas and 59 Cyg are typical for a pole-on Be star disk with a low $v \sin i$ value, while the shell spectrum cannot be distinguished from that of a large $v \sin i$ Be star. Shell emission lines can be explained by circumstellar disks, seen nearly edge-on. Both stages, broad and narrow line, are atypical for a Be star with $v \sin i = 300$ km s^{-1}. Both observed line width stages are in contradiction with a circumstellar disk seen at about $i = 45°$.

Our new proposal is based in the following argument: The similarity of both the narrow-line profiles of γ Cas with those of ordinary pole-on Be stars and the broad-line profiles with those of ordinary Be shell stars led us to retain the kinematical structure of a circumstellar rotating disk. But we no longer assume that the disk is located in the equatorial plane of the central star. We postulate the following two properties for the circumstellar disk, valid during the epochs of SV:

1. The emission lines of γ Cas are produced in a circumstellar rotating disk tilted with respect to the equatorial plane of the central star.
2. The ascending node Ω of the circumstellar orbits is precessing around the central star.

The precessing of the nodal line could be a natural consequence of perturbations in the gravitational field, such as rotational deformation of the central star.

The rotation axis of the disk precesses around the rotation axis of the central star and a cyclic variation of the disk inclination i_{d} becomes apparent (Fig. 2). In this way it is possible to identify the slightly kinematically broadened narrow-line stage with a nearly pole-on disk and the largely kinematically broadened shell stage with a nearly edge-on disk, while the stellar rotation axis remains unchanged and the stellar $v \sin i$ remains constant during the precession of the nodal line.

In applying this idea to γ Cas we assume, that there was an equatorial disk until 1934 (epoch A), which then started to tilt when the SV began (epoch B). The disk vanished in 1940 (most probabebly re-accreted by the central star) which is documented by the absence of emission lines in that period. After 1940, a new circumstellar (ordinary, untilted) equatorial disk was generated which is still present.

4. Some tests of the postulates

In the following we will first derive some consequences of a tilted-disk model and compare these predictions with the observations in order to obtain the limits of our hypothesis. Questions concerning the stability and the origin of the tilt will be discussed in Sect. 5.

4.1. The emission disk radius R_{d}

The emission lines, observed by Baldwin are mainly broadened due to the kinematics of the tilted disk. Electron scattering (Poeckert & Marlborough 1979) and non-coherent scattering broadening (Hummel 1994) do not play a rôle in Hδ. Emission disk radii of equatorial rotating disks, expressed in units of the stellar radius R_{d}/R_*, are usually calculated by using the peak separation of double-peak profiles, normalized to the stellar $v \sin i$ (Huang 1972). This approach is no longer valid for a tilted disk, because the stellar rotation $v \sin i$ and the rotation of the circumstellar disk have different projections. In order to test if the outer disk radius was nearly constant or varied the peak

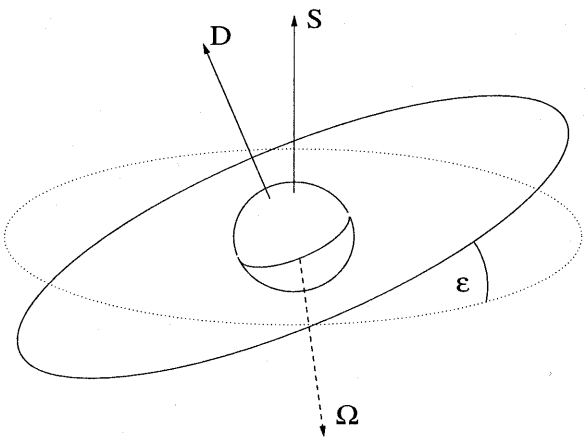

Fig. 2. Sketch of a tilted circumstellar disk. ϵ is the tilt angle of the disk with respect to the equatorial plane of the star (dotted). Ω is the node line. 'S' refers to the stellar rotation axis and 'D' refers to the rotation axis of the disk.

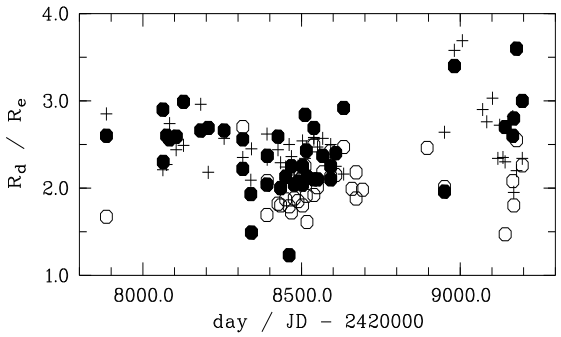

Fig. 3. Emission disk radii R_d expressed in units of the radius derived from the ΔV_edge values, computed be means of Eq. (5) and Table 3, 4 and 5 of Baldwin (1939). Full circles indicate Hδ, open circles are for He I and crosses are for Fe II emission lines.

separation ΔV_peak could be expressed in units of the total width of the line profiles ΔV_tot. The ratio of

$$\frac{R_\mathrm{d}}{R_\mathrm{i}} = \left(\frac{\Delta V_\mathrm{tot}}{\Delta V_\mathrm{peak}}\right)^2 \tag{2}$$

is independent of the inclination for a rotating disk because the projection cancels out. R_i in Eq. (2) is the inner emission disk radius. On the other hand, if the documented emission line variations are due to a change in the emission disk radius R_d alone one would expect a minimum of $R_\mathrm{d}/R_\mathrm{i}$ at the shell stages and larger values near the single-peak stages.

The bottom widths ΔV_tot of the emission lines are not provided by Baldwin (1940), but the emission edge. The emission edge V_edge is (according to Baldwin's Fig. 2) measured in the wing of the emission line profile and is closer to the radial velocity at the half mean of the profile. Therefore the separation of both V_edge measurements

$$\Delta V_\mathrm{edge} = V^\mathrm{r}_\mathrm{edge} - V^\mathrm{b}_\mathrm{edge} \tag{3}$$

is a value between the FWHM and ΔV_tot:

$$\mathrm{FWHM} < \Delta V_\mathrm{edge} < \Delta V_\mathrm{tot} \tag{4}$$

This interpretation of ΔV_edge is also supported by comparison of Baldwin's values of ΔV_edge with FWHM and ΔV_tot values of γ Cas obtained recently in 1993 (Hummel & Vrancken 1995). γ Cas shows a FWHM of 310 km s^{-1} for the three optical emission lines Hα, He I λ5876 and Fe II λ5317, in agreement with Cleminshaw's data for ΔV_edge, while ΔV_tot of the He I and Fe II emission lines exceed 500 km s^{-1}.

Consequently a disk radius ratio defined by

$$\frac{R_\mathrm{d}}{R_\mathrm{e}} = \left(\frac{\Delta V_\mathrm{edge}}{\Delta V_\mathrm{peak}}\right)^2 \tag{5}$$

reacts to changes in inclination and disk radius in the same way as $R_\mathrm{d}/R_\mathrm{i}$ but with a smaller amplitude.

Relative disk radii $R_\mathrm{d}/R_\mathrm{e}$ are given in Fig. 3 as a function of time covering both shell phases and the last single-peak stage. During the second narrow-width single-peak stage the emission peaks are no longer resolved, and relative disk radii cannot be derived. Taking into account the statistical errors and the large sensitivity of $R_\mathrm{d}/R_\mathrm{e}$ on the radial velocities one must conclude that the emission disk radius was constant in all three emission lines between t = 7885 and t = 9196. The He I emission region was probabebly somewhat smaller during the two shell stages. The nearly constant value of $R_\mathrm{d}/R_\mathrm{e}$ is in agreement with the assumption of nearly constant emission radius for Hδ, Fe II and He I during epoch B. Moreover, the idea that SV are mostly due to a variation of the disk size (R_d) can be ruled out.

4.2. Period of ascending node motion P_Ω

The two shell stages are separated by about 1450±140 days. The separation of both narrow-line stages is better determined by 1014 days±10 days. The uncertainties of the shell stage separation is mostly due to the unknown maximum of the second shell phase, since the emission faded. The uncertainty of the separation of the narrow line stages is mostly due to the poor time resolution of the first narrow line epoch, which was observed almost every 100 days, while the second narrow line stage was monitored with a much smaller time interval of $\Delta t \simeq 10$ days. If the SV are only due to a secular motion of the ascending node, the phase difference between a narrow-line stage and a shell phase is $\Delta\Omega = \pi$ and the phase difference between two shell-phases or two single-peak phases indicate a full period of the node line: $\Delta\Omega = 2\pi$ (see also Table 1). The evolution of P_Ω is displayed in Fig. 5, it shows a linear increase in time, which implies a slow down of the node line motion.

4.3. Tilt angle ϵ

Now we turn to the evolution of V_edge. As a first step we derive the theoretical Keplerian velocity at $r = R_*$ for a B0 IV star (Hoffleit & Jaschek 1982) with mass $M_* = 26 M_\odot$, radius $R_* = 11.6 R_\odot$, and log g = 3.9 (Allen 1973) to be $V_\mathrm{K}(R_*) = 654$ km s^{-1}, which

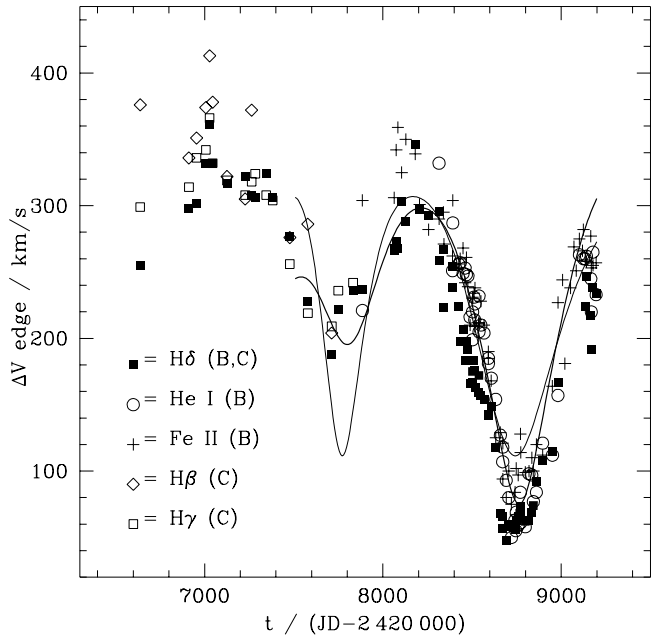

Fig. 4. The evolution of $\Delta V_{\rm edge}$ of different emission lines covering 20 years. (B)=Baldwin (1941); (C)=Cleminshaw (1936). Two predicted $\Delta V_{\rm edge}$ curves are overplotted. Thin line: the tilt angle ϵ is assumed to be constant. The bold line is for a tilt angle linearly increasing with time (see Eq. (4))

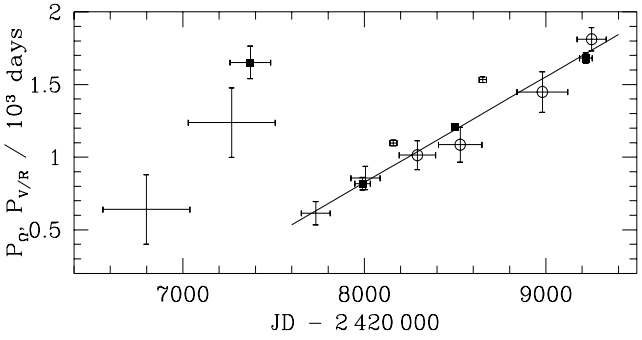

Fig. 5. Evolution of the node period P_Ω (circles) and of the apsidal period $P_{\rm V/R}$ (dots and squares). Full squares are based on $V = R$ phases, dots are based on phases with extrema of V/R-ratio.

corresponds to a revolution time of $t_{rev} = 21.5h$. Assuming an inclination of $i = 45°$ (Quirrenbach et al. 1993) the unprojected equatorial rotation velocity of about 420 km s^{-1} can be derived from $v \sin i$ = 300 km s^{-1}; 65% of the Keplerian value at $r = R_*$.

The apparent inclination of the tilted disk $i_{\rm disk}$ differs from that of the star i_* and can be derived from spherical trigonometry

$$i_{\rm disk}(\Omega) = \arccos\left[\cos\Omega \sin\epsilon \sin i_* + \cos\epsilon \cos i_*\right] \quad (6)$$

In Sect. 3.1 we argued that the variations in $\Delta V_{\rm edge}$ are mostly due to the variation of the disk inclination $i_{\rm d}$ given by Eq. (6) and are not due to a change in the emission radius $R_{\rm d}$. On the other hand $\Delta V_{\rm tot}(t)$ is related to the disk inclination via

$$V_{\rm tot}(t) = 2V_{\rm K} \sin\left(i_{\rm disk}(\Omega(t))\right). \quad (7)$$

Because the measured values $\Delta V_{\rm edge}$ are smaller than the total profile widths, we adopt the same relation for $\Delta V_{\rm edge}$:

$$V_{\rm egde}(t) = 2kV_{\rm K} \sin\left(i_{\rm disk}(\Omega(t))\right). \quad (8)$$

where $k = (\Delta V_{\rm edge}/\Delta V_{\rm tot}) < 1$. Fig. 4 shows $\Delta V_{\rm edge}$ as a function of time t as derived from different emission lines. We fitted all data with $t > 7600$ using Eqs. (8), (6), and (11). The best fit parameters are $\epsilon = 25°$ and $2kV_{\rm K}$ = 326 km s^{-1} with $\chi^2 = 5$.

The comparison with observations (Fig. 4) clearly indicates, that the first narrow stage is much less developed, than the second narrow stage. This could be partly due to the different systematic errors in $\Delta V_{\rm edge}$ for $t > 8000$ and for $t < 8000$ as discussed in Sect 4.1. However, Baldwin's sequence of Hδ line profile shapes shows the second single peak much better developed with a peak intensity of about 4 F_c than the first single peak stage with $I = 1.3 \ldots 1.4F_c$, giving rise to the fact, that the different systematic errors are of minor importance. Therefore the differences in both single-peak stages are real. According to our model this would mean an increase of the tilt angle ϵ with time. We therefore allow a linear dependence of ϵ on the time:

$$\epsilon(t) = \dot\epsilon(t - t_0) \quad (9)$$

The best fit values for such a fit are $\dot\epsilon = 2.36 \times 10^{-2} \frac{\rm deg}{\rm day} = 1.42 \frac{\rm arcmin}{\rm day}$, $2kV_{\rm K}$ = 330 km s^{-1} and $t_0 = 7406$ with a lower $\chi^2 = 2.9$. The tilt would be $\epsilon(t = 8799) = 33°$ at the second single-peak stage, meaning a disk inclination of $i_{\rm d} = 12°$. The results are shown in Fig. 4, where the bold curve gives the expected line width variation for a linearly increasing tilt angle. The cyclic pattern of $\Delta V_{\rm edge}$ for $t > 7600$ is well reproduced. Also the tilt starting date of $t \simeq 7400$ coincide with the period drop in Fig. 5.

4.4. V/R-variations and P_ω

Apart from the cyclic variations of the emission line width discussed above, both γ Cas and 59 Cyg showed cyclic V/R-variations, in such a manner, that V/R was greater than 1 from shell to single-peak phase and less than 1 from the single-peak to the shell phase. Since V/R-ratio variations in Be stars can be understood in terms of a perturbation, superimposed on an axisymmetric, equatorial Keplerian disk (Okazaki 1991; Telting et al. 1994; Hummel & Hanuschik 1997), we assume analogous, that V/R-ratio variations during SV can be approximated as a perturbation in the density and velocity distribution superimposed on a axially symmetric tilted circumstellar disk.

Symmetric Hδ emission lines are observed near $t = 6201 \pm 200$, $t = 6959 \pm 150$, $t = 7785 \pm 75$ (narrow line stage), $t = 8194 \pm 10$, (shell stage) $t = 8799 \pm 10$ (narrow-line stage), and near $t = 9640 \pm 60$ (shell stage). In both narrow-line and shell stages, the V/R asymmetry changed sign. The evolution of $P_{\rm V/R}$ is shown together with P_Ω in Fig. 5, where

we have distinguished between $P_{\rm V/R}$ values derived from intervals between symmetric phases ($V = R$) and those derived from intervals between phases of largest asymmetry V/R. For $t < 7400$, the V/R-ratio cycle period slowly increases. Around $t = 7400 \ldots 7600$, when the emission line width variations began, $P_{\rm V/R}$ suddenly drops to the value it had several years previously, when the V/R-ratio variation began. As Fig. 5 indicates, $P_{V/R}$ and P_Ω increase linearly with time until the emission fades and the disk disappears. For $t > 7600$ we find the linear fit:

$$P_\Omega, P_{V/R} = 0.7282 \times t - (5000 \pm 3500) \tag{10}$$

Integration yields:

$$\Omega(t) = 8.6284 \ln\left(P_\Omega(t)\right) - \Omega_0 \tag{11}$$

$\Omega(t = 8799) = \frac{\pi}{2}$.

Since the present 'normal' V/R-ratio variations also exhibit an increasing cycle time (Doazan et al. 1987a), we fit the time interval from $t = 20500$ to $t = 26500$ (1969-1985) in the same way and found[1]

$$P^{\rm n}_{V/R} = 0.422 \times t + (540 \pm 328). \tag{12}$$

This means that the present linear cycle time increase is a factor

$$\frac{\dot{P}^{\rm n}_{V/R}}{\dot{P}_{V/R}} = 0.58 \tag{13}$$

slower than in epoch B.

Despite this remarkable difference we argue for a global density wave (Okazaki 1991) as the underlying cause of the V/R-variations:

- For γ Cas the V/R-ratio variations began already in 1928, several years before the first narrow-line phase. In this epoch A (1928-1934) the V/R-ratio variations are indistinguishable from normal long-term V/R-ratio variations.
- Both cycle times $P_{\rm V/R}$ and $P^{\rm n}_{V/R}$ exhibit the same evolution, they increase linearly with time.
- The strongest argument, however, comes from the observed line profile shift. Baldwin (1940) reported that during the V/R-variations the photospheric absorption in the Hδ line profile 'is strengthened on the side adjacent to the stronger emission component'. This means that the asymmetric emission line is shifted towards the direction of the fainter emission peak with respect to the photospheric absorption, an effect frequently observed in optically thin emission line profiles of other long-term V/R-variable Be stars, as well as in γ Cas itself during its present state of long-term V/R-variability (Doazan et al. 1983; Hummel & Vrancken 1995).

[1] Telting & Kaper (1994) fitted the 'normal' V/R-ratio variations (1969-1989) to an analytic expression, non-linear in $P(t)$. The linear part of their fit would correspond to $P^{\rm n}_{V/R} = 0.364 \times t + 790$.

We therefore identify $P_{V/R}$ with the precession period of the perturbation pattern P_ω.

A final point to consider is the fact that He I emission lines exhibit width variations but no V/R-ratio variations and that the V/R-ratio variations of the Fe II emission lines of multiplets $b^4P\text{-}z^4D^0$ and $b^4F\text{-}z^4D^0$ preceded those of Hδ by about 150 days, giving rise to a more complex circumstellar perturbation pattern. In particular, the He I lines indicate that the innermost regions were tilted, but still axisymmetric, and the phase lag between Fe II and Hδ suggests a possible differential precession in the perturbation pattern.

4.5. Satellite theory

The evolution of a tilted disk in a perturbed gravitational field has been studied e.g. by Papaloizou & Terquem (1995). Since we do not know the source of the tilt in γ Cas and 59 Cyg we compare our findings with the known evolution of an elliptical tilted ring.

The fast stellar rotation causes a flattened surface implying no longer a spherically symmetric gravitational field U. We assume that U is rotationally symmetric and symmetric with respect to the equatorial plane. Such a potential can be expanded in terms of Legendre polynomial (e.g. Chebotarev 1967, chap. 4.2; Roy 1988, chap. 10.4; Stumpff 1965, chap. XXII). The first order secular perturbations of the orbital parameters $\omega(t)$ and $\Omega(t)$ are well known

$$\dot{\Omega} = -J_2 \left(\frac{R_*}{a}\right)^2 \frac{\cos(\epsilon)}{\left(1 - e^2\right)^2} \tag{14}$$

and

$$\dot{\omega} = \frac{1}{2} J_2 \left(\frac{R_*}{a}\right)^2 \frac{5\cos^2\epsilon - 1}{\left(1 - e^2\right)^2} \tag{15}$$

while the eccentricity e, the tilt ϵ and the semi-major axis a are only subject of short-term periodic perturbations. In Eqs. (14) and (15) $J_{\rm n=2}$ is a function of the moments of inertia of the flattened star. Note that ω is the angle between the periastron and the precessing node line Ω. For our purpose we give

$$\dot{\tilde{\omega}} = J_2 \left(\frac{R_*}{a}\right)^2 \frac{1 - \frac{3}{2}\sin^2\epsilon}{\left(1 - e^2\right)^2} \tag{16}$$

where $\tilde{\omega}$ is the angle between periastron and a fixed direction in the equatorial plane and is directly related to observed V/R-ratio cycle time.

We will use this approach only for qualitative arguments. In application to γ Cas we have to keep in mind, that Eqs. (14) and (16) predict differential precessing in a radially extended disk causing circularisation of the orbits, widening of the disk height and particle interactions, while we can expect to obtain reliable results only for circumstellar rings with a small radial extension ($\Delta R \ll a$).

The current approach of satellite orbits around oblate stars ($J_2 \neq 0$, $J_{n>2} \ll J_2$) can also not give an explanation for the

tilt and its increase. For the following we neglect the influence of possible higher order moments ($n > 2$) on $\dot{\Omega}$ and $\dot{\omega}$.

For small values of ϵ there is

$$\dot{\Omega} = -\dot{\tilde{\omega}} \tag{17}$$

implying equal speed of Ω and $\tilde{\omega}$ in opposite direction. The observed equality of $P_{V/R}$ and P_Ω (Fig. 5) is in agreement with a rather small tilt angle.

Concerning the direction of $\dot{\Omega}$ and $\dot{\omega}$, the observations are two folded. Setting $\Omega = 0°$ for the observers direction projected to the equatorial plane, we can immediately set $\Omega = \frac{3\pi}{2}$ for the pole-on stage and $\Omega = \frac{\pi}{2}$ for the shell-stage. For clock-wise rotation of the elliptical orbits we can identify $V \ll R$ with $\tilde{\omega} = \frac{3\pi}{2}$ and $V \gg R$ with $\tilde{\omega} = \frac{\pi}{2}$ (Table 1). However a further constraint to determine the direction of $\dot{\tilde{\omega}}$ with respect to $\dot{\Omega}$ cannot be extracted. Therefore the observations are in agreement with $\dot{\tilde{\omega}} = -\dot{\Omega}$ and with $\dot{\tilde{\omega}} = \dot{\Omega}$ with a constant phase shift of $\tilde{\omega} - \Omega = \frac{3\pi}{2}$. While the first possibility does fit a low-tilt elliptical precessing ring, the latter possibility requires an unrealistic large tilt angle of $\epsilon = 70.53°$.

A final point to note is that, in the frame of a tilted elliptical ring, the decreasing $\dot{\Omega}$ and $\dot{\tilde{\omega}}$ can be either a consequence of a slowly increasing tilt angle ϵ and/or a circularisation of the elliptic orbits ($e < 1 \rightarrow 0$).

4.6. Comparison with the visual light-curve

In a final step we compare our findings concerning the emission lines with the photometric variations of γ Cas . Telting et al. (1993) argue that the Paschen continuum is partially optically thick since 1970 during the normal V/R-ratio variations. They conclude that the continuum energy distribution is not very sensitive to the deviations of the axisymmetry in the disk. If the Paschen continuum of the disk was also partially optically thick during the SV we can expect visual brightness variations due to different projections of the continuum emitting disk surface. The photometric light-curves of Huffer (1938) and Howarth (1979) are collected in Fig. 6. The maximum in the V-band light curve at t=8662 coincides with the phase of the line widths minimum which precedes the line intensity maximum by about 140 days. A possible second brightening, only visible in Huffers light-curve, occurs around t=9120.

The pre-outburst magnitude of $V = 2\overset{\mathrm{m}}{.}1$ consists of the stellar brightness I_* and that of the untilted disk $I_\mathrm{d}\cos(i_\mathrm{d} = 45°)$; the post-outburst magnitude of $V = 2\overset{\mathrm{m}}{.}8$ is the pure stellar brightness after the disk has vanished. With these constraints we apply

$$m_V = 2\overset{\mathrm{m}}{.}8 - 2.5\log\left(\frac{I_* + I_\mathrm{d}\cos i_\mathrm{d}}{I_*}\right). \tag{18}$$

We thereby neglect circumstellar limb darkening and the fading of the circumstellar disk. The corresponding light-curve is shown in Fig. 6.

The comparison shows that the decreasing brightness after the second single-peak phase can be understood by the fading

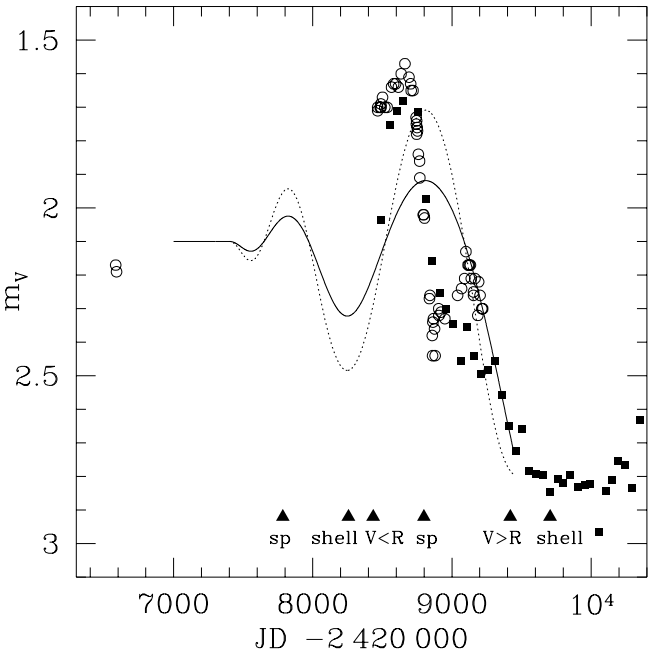

Fig. 6. Photometric light-curve in the V-band of Huffer (1938) (O) and Howarth (1979) (■). The solid line is for a disk with a tilt angle linearly increasing with time (see Eq. (9)). The dotted curve is for the same model, except we used a simple limb darkening $\sim \cos i_\mathrm{d}$ for the circumstellar disk. The arrows indicate significant phases of the emission lines.

of the disk and the increasing disk inclination. The observed V-band maximum is larger than predicted by the model. We therefore applied a simple limb darkening for the circumstellar Paschen continuum $\sim \cos i_\mathrm{d}$. Such a model matches better the light-curve maximum. However, the photometric brightening clearly precedes the pole-on phase predicted by the variations of the emission lines alone. This result again gives rise to a more detailed structure of the circumstellar disk, probabebly due to differential precession of the nodal line and the apsidal line.

5. Discussion

The last and most pressing question is the origin of the tilt itself. There are several possibilities, but the observations do not reveal any indication as to what could give rise to a tilt of a circumstellar disk. Thus the following discussion is tentative.

The only useful observation in this context is the sudden drop of $P_{\mathrm{V/R}}$ of about a factor of 3 around $t \simeq 7400$ which coincides with the beginning of the line width variations. Since that time ϵ was increasing, hence there must have worked a permanent force asymmetric with respect to the equatorial plane during epoch B.

Speaking in terms of orbits around an oblate star, an increasing tilt angle requires an additional $n = 3$ moment in the gravitational field ($J_3 \neq 0$). Since there is no observational evidence for SV after 1940, such a $n = 3$ moment is no longer active.

We will not discuss the possibility of a gravitational $n = 3$ moment originating in the central star, but limit the discussion on external gravitational sources.

5.1. Close encounter

A close encounter scenario by an unbounded stellar body provides a single event in the sense of a temporary $n = 3$ moment. Star-disk interactions have been studied for T Tauri stars, which are embedded in a dense cloud of a star forming region. SPH calculations by Heller (1993) indicate that massive encounters can indeed result in disk tilts of about $\epsilon = 20°$ for a larger range of parameters.

Since neither γ Cas nor 59 Cyg belong to an open cluster the encounter probability is very small. Tests could be the radial velocity of the Be-star before and after the event, which should be different for advantageous perspectives. Unfortunately, there are no radial velocity measurements from stellar absorption profiles of γ Cas before the SV.

5.2. γ Cas as a binary

γ Cas is known to be an X-ray source (Mason et al. 1976) with a strong hardness ratio of $HR = 0.871$ (Berghöfer et al. 1996) typical for a Be/X-ray binary (Rappaport & van den Heuvel 1982). Recently, Haberl (1995) found the soft component of the X-ray spectrum to be variable. The X-ray source could be either a neutron star or more probabebly a white dwarf. However, no period has been found yet which could be associated with an orbital period of a binary. If these observations indicate that γ Cas is a Be/X-ray binary, one can speculate that the orbital plane is not coplanar with respect to the equatorial plane. Hence an eccentric orbit with a period of $P > 70$ years (according to the emission line detection of γ Cas in 1866 and the start of SV in 1934) would induce a temporary external perturbing field with a $n = 3$ moment resulting in an increasing disk tilt during the time of closest approach (= epoch B). The evolution of the disk of γ Cas is then determined by the stellar flattening and the external perturber.

Recent theoretical studies on the dynamics of circumstellar disks in binary systems (e.g. Papaloizou & Terquem, 1995) show, that circumprimary discs are generally able to adjust as a rigid body to a new equilibrium, and need not necessarily be disrupted. Since the disk precession speed at $R = 3R_*$ of $V_\Omega = 1.7$ km s^{-1} is much lower than the sound speed of $V_s \simeq 12$ km s^{-1} for $T = 10\,000$ K, the circumstellar gas of γ Cas can respond on the perturber via a density wave.

Though we do not know the exact perturbation profile of the density and the velocity in the disk of γ Cas , the theoretical studies generally support the idea of a tilted disk as the cause of cyclic emission line width variations.

In this context it would be worthwhile to compare the SV of γ Cas with emission line variations of other Be/X-ray binaries during X-ray outbursts, when the compact object interacts with the circumstellar environment.

5.3. Interactions between the stellar wind and the circumstellar disk

There are open fundamental questions concerning the formation of 'normal' Be stars disks. If the central star loses mass in an episodic manner followed by a low-viscosity re-accretion as does μ Cen (Hanuschik et al. 1993) we can speculate that the inner regions of the disk can only be tilted during a mass-loss quiet epoch. If we believe in a stationary low-velocity equatorial outflow (e.g. Waters & Marlborough 1994) a tilt will never evolve to the inner parts, hence the disk will most probabebly warped.

Be stars have strong circumstellar winds with $V_\infty = 500 - 1\,000$ km s^{-1} . The observations (UV, optical, IR) show, that both circumstellar disk and stellar wind co-exist and evolve independently of each other. Recent hydrodynamical studies of Owocki et al. (1996) have shown that the non-radial line-forces and limb darkening in the rotating wind do not lead to the wind-compressed disk scenario as proposed by Bjorkman & Cassinelli (1993) rather they induce a density void in the equatorial region around the star.

With regard to our hypothesis of a circumstellar disk tilted with respect to the rotation axis of the wind, we can expect, that a rotating wind will push a tilted disk back to the equatorial plane of the star within $R \lesssim 2R_*$, independent of the assumed mass-loss scenario.

5.4. Self-induced warping

In a recent study, Pringle (1996) demonstrated that disks around luminous objects can be warped due to the radiation pressure. He derived a lower limit radius, for which the disk can become unstable (his Eq. 4.4). Applying this to B-type stars ($M_* = 26M_\odot; R_* = 12R_\odot$) and assuming an isotropic distribution of the circumstellar viscosity ($\eta = 1$) we derive $R/R_* = 10^7$, much larger than typical circumstellar disk radii of Be stars. Self induced warping due to radiation pressure is therefore not likely to account for the disk tilt.

6. Conclusions

Spectacular variations, which have been observed in two Be stars, γ Cas and 59 Cyg, have been investigated. Based on the striking emission line *width* variation we argued for a circumstellar disk to be tilted with respect to the equatorial plane of the central star. The hypothesis has been tested in some aspects. Our main findings are

- Variations of the disk scale height H, the meridional opening angle Θ, the disk radius R_d or the circumstellar kinematics alone cannot account for SV.
- If SV are due to a variation of the disk inclination, the observed variation of the peak separation is in agreement with a constant emission disk radius.
- The evolution of ΔV_edge (corresponding to a value between FWHM and ΔV_tot) can be fitted by a simple kinematical model of a disk with increasing tilt angle.

– Since a) the combined evolution of $\Delta V_{\rm edge}(t)$ and V/R (t) can be understood in terms of a narrow eccentric tilted ring, precessing in the gravitational field of a rotationally flattened star and since b) the asymmetric emission lines of γ Cas show the same profile shift behavior as asymmetric line profiles of Be stars with normal V/R-ratio variations, we argue for a global m = 1 disk oscillation pattern in a tilted disk.
– Assuming an optically thick Paschen continuum the predicted photometric variations are a reasonably good match to the observed visual light curve and therefore tentatively support the kinematical interpretation of SV.
– The analyzed data are insufficient to derive constraints on the origin of the tilt. Since a) the evolution of the disk tilt requires an additional temporary gravitational perturbation, which is no longer symmetric with respect to the equatorial plane and since b) γ Cas is supposed to be a Be/X-ray binary with unknown orbital parameters, we favorite a scenario, where the tilt is induced by a secondary in a non-coplanar eccentric orbit.

We stress that the comparison with high-resolution observations of optical emission lines from known Be/X-ray binaries during their X-ray outburst will reveal the origin of SV in Be stars and its possible relation to binarity.

Acknowledgements. Financial support by the *Service Centres and Research Networks* initiated and financed by the Belgian Federal Scientific Services (DWTC/SSTC; SC/005) and the *Deutsche Forschungsgemeinschaft* (Ku 447/22-1) is gratefully acknowledged. We thank the referee, R. Waters, for his constructive criticisms of the manuscript. This research made use of the Simbad database, operated at CDS, Strasbourg, France.

References

Allen C.W., 1973, *Astrophysical Quantities*, third edition, Athlone, London
Baldwin R.B., 1939, ApJ 89, 255 (B1)
Baldwin R.B., 1940, ApJ 92, 82 (B2)
Baldwin R.B., 1941, ApJ 93, 333 (B3)
Barbier D., 1948, Ann. Astrophys. 11, 13
Barker P.K., 1982, ApJS 49, 89
Beekmans F., 1976, A&A 52, 465
Berghöfer T.W., Schmitt J.H.M.M., Cassinelli J.P., 1996, A&AS 118, 481
Bjorkman J.E., Cassinelli J.P., 1993, ApJ 409, 429
Chebotarev G.A., 1967, *Analytical and Numerical Methods of Celestial Mechanics*, Elsevier, New York
Cleminshaw C.H., 1936, ApJ 83, 495
Dachs J., 1987, in IAU Coll. 92, p149
Doazan V., 1975, A&A 8, 148
Doazan V., Franco M., Rusconi L., Sedmak G., Stalio R., 1983, A&A 128, 171
Doazan V., Franco M., Rusconi L., Sedmak G., Stalio R., 1987, ESA SP-1147
Doazan V., Rusconi L., Sedmak G., Thomas R.N., Bourdonneau B., 1987a, A&A 182, L25
Doazan V., Barylak M., Rusconi L., et al., 1989, A&A 210, 249
Doazan V., De La Fuente A., Cramer N., Barylak M., 1994, in IAU Coll. 162, p360
Edwards D.L., 1944, MNRAS 104, 283
Edwards D.L., 1956, Vistas in Astronomy 2, 1470
Goraya P.S., Tur N.S., 1988, Ap&SS 145, 263
Greaves W.M.H., Martin E., 1936, ApJ 98, 434
Gulliver A.F., 1977, ApJS 35, 441
Haberl F., 1995, A&A 296, 685
Hanuschik R.W., 1987, A&A 173, 299
Hanuschik R.W., 1996, A&A, 308, 170
Hanuschik R.W., Dachs J., Baudzus M., Thimm G., 1993, A&A 274, 356
Hanuschik R.W., Hummel W., Dietle O., Sutorius E., 1995, A&A 300, 163
Heller C.H., 1993, ApJ 408, 337
Hirata R., Kogure T., 1978, PASJ 30, 601
Hoffleit D., Jaschek C., 1982, *The Bright Star Catalogue*, fourth Ed., Yale University Observatory, New Haven, Connecticut
Howarth I.D., 1979, J. Brit. astron. Assoc. 89, 378
Huang S.S., 1972, ApJ 171, 549
Hubert A.M., 1994, in IAU Symp. 162, p341
Hubert-Delplace A.M., Hubert H., 1981, A&AS 44, 109
Huffer C.M., 1938, ApJ 89, 139
Hummel W., 1994, A&A 298, 458
Hummel W., Hanuschik R.W., 1997, A&A 320, 852
Hummel W., Vrancken M., 1995, A&A 302, 571
Kogure T., Hirata R., Asata W., 1978, PASJ 30, 385
Kogure T., Hirata R., 1982, BAS India 10, 281
Lockyer W.J.S., 1933, MNRAS 93, 362, 619
Marlborough J.M., 1997, A&A 317, L17
Marlborough J.M., Snow T.P., 1980, ApJ 235, 85
Mason K.O., White N.E., Sanford P.W., 1976, Nat 260, 690
McLaughlin D.B., 1937, ApJ 85, 181
Okazaki A.T., 1991, PASJ 43, 75
Owocki S.P., Cranmer S.R., Gayley K.G., 1996, ApJ 472, L115
Papaloizou J.C., Savonije G.J., Henrichs H.F., 1992, A&A 265, L45
Papaloizou J.C.B., Terquem C., 1995, MNRAS 274, 987
Poeckert R., Marlborough J.M., 1978, ApJ 220, 940
Poeckert R., Marlborough J.M., 1979, ApJ 233, 259
Pringle J.E., 1996, MNRAS 281, 357
Quirrenbach A., Hummel C.A., Buscher D.F., et al., 1993, ApJ 416, L25
Rappaport S., van den Heuvel E.P.J., 1982, in IAU Symp. 98, p327
Roy A.E., 1988, "Orbital motion", third edition, Hilger, Bristol
Secchi A., 1867, Astron. Nachr. 68, 63
Slettebak A., Reynolds R.C., 1978, ApJS 38, 205
Struve O., 1931, ApJ 73, 94
Stumpff K., 1965, *Himmelsmechanik II*, VEB, Leipzig
Telting J.H., Kaper L., 1994, A&A 284, 515
Telting J.H., Waters L.B.F.M., Persi P., Dunlop S.R., 1993, A&A 270, 355
Telting J.M., Heemskerk M.H.M., Henrichs H.F., Savonije G.J., 1994, A&A 288, 558
Waters L.B.F.M., Marlborough J.M., 1994, in IAU Coll. 162, p399